Depth and Detours: An Essay on Visually Guided Behavior*

Michael A. Arbib
and
Donald H. House

Computer & Information Science Department
University of Massachusetts
Amherst, Massachusetts 01003

COINS Technical Report 85-28

---

*The research reported in this paper was supported in part by the National Institutes of Health under grant no. NS14971-04.

Depth and Detours: An Essay on Visually Guided Behavior[1]

Michael A. Arbib
Center for Systems Neuroscience,
Computer & Information Science Dept.
University of Massachusetts
Amherst, MA 01003

Donald H. House
Department of Mathematical Sciences
Williams College
Williamstown, MA 01267

ABSTRACT

Motivated by data on the way in which a toad will sidestep around a barrier to get to prey, we offer a number of alternative models for the neural networks underlying such phenomena. First, we introduce a one-dimensional model, and then compare it to experiments which show that the animal must make use of the depth of objects in determining its course of action. On this basis, we review earlier work on depth perception in toad. We then turn to two models for the use of this information in detour behavior. The first builds on the one-dimensional model to indicate how the animal might 'choose' to turn to the end of a barrier or directly towards a worm. The second model indicates how the animal might come to represent in its head trajectories or a series of landmarks which can determine an overall path of action, rather than a single initial target.

[1] The research reported in this paper was supported in part by the National Institutes of Health under grant no. NS14971-04.

1. Introduction

This paper is one of a series in which we build neural models of visuomotor coordination in frog and toad to exemplify the style of neural processing which involves dynamic parallel interaction between layers of neurons, rather than a simple stimulus-response chain or a control action which can be adequately represented in terms of lumped models. Amongst the earlier studies in this series are those of pattern recognition, which indicate how a neural network can take a spatial array of stimulation to tell prey from predator (Lara, Cervantes, and Arbib, 1982; Cervantes, Lara, and Arbib, 1985), and a model of prey selection in which we explain possible mechanisms for how an animal, confronted with a spatially structured environment containing several prey objects, will come to snap at only one of them (Didday, 1976; Lara, and Arbib, 1982). In the present paper we move beyond models of the recognition of visual patterns that serve to trigger stereotyped, though appropriately spatially directed, responses and instead consider situations in which the animal exhibits behavior which takes account of a complex spatial context. Specifically, we shall start from data on a toad viewing a vertical paling fence behind which there is a worm. It has been shown that the animal may either snap directly at the worm, or may detour around the barrier. However, it will not go around the barrier if there is no worm behind it. Thus, we may still see the worm as triggering the animal's response, but we no longer see only the stereotyped snap directly at the worm, but rather a complex trajectory dependent upon the relative spatial position of worm and barrier.

A first view of these data is given in Figure 1, from Collett (1982) – more data will be reviewed in Section 3. The row of dots indicates a paling fence. The two circles indicate two alternative placements of worms which are to attract a toad's attention, while the T indicates an opaque barrier which prevents the toad from seeing the worms after it has moved from the start position. The position of the toad is represented by a dot for its head and a line for its orientation. The sequence of such 'arrows' on the right-hand side of the figure indicates successive positions taken by the toad in a single approach to the prey. The animal sidesteps around the barrier, pauses for several seconds, and then continues to a position at which it stops, pointing in approximately the direction of the worm – but note that, due to the opaque barrier, the worm is no longer visible. On the left-hand side of the figure, we indicate the position of the toad on a number of different occasions, at the pause. The dashed arrows correspond to the nearer position for the worm, the solid arrows correspond to the position of the pause for the further position. What is of interest is that even though the worms are no longer visible to the toad at the time of the pause, the orientation of the animal correlates well with the position of the target. Thus, we must not only explain how it is that the animal chooses whether to proceed directly toward the prey or to sidestep around the barrier, but also come to understand how the position of the target can be encoded in such a way as to be available to guide the animal's behavior even if the target does not continue to be visible.

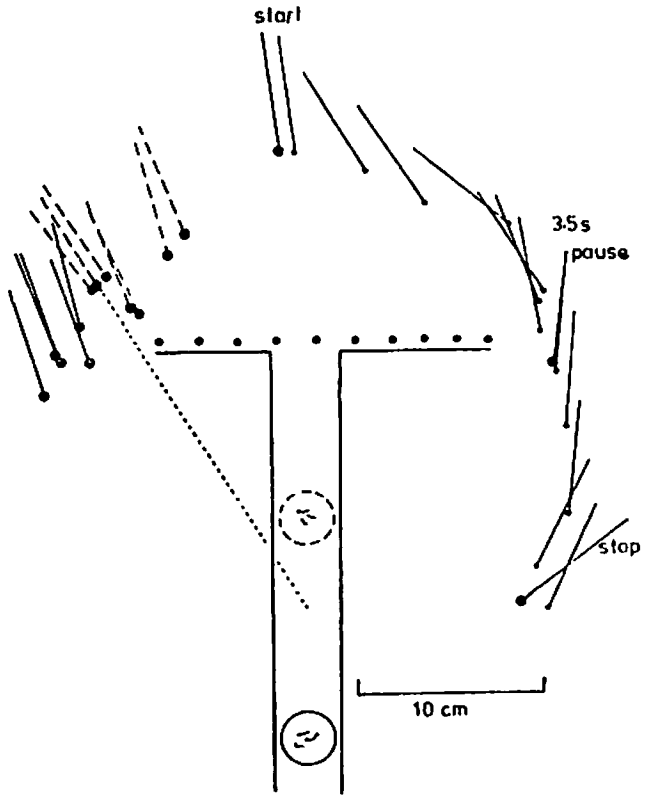

Fig. 1 – Toad Trajectories

Results of several experiments involving a toad's approach to prey behind an occluding barrier. Solid lines to the right indicate the orientation of the body axis of a toad and its snout position (dots) at intervals along its path towards the prey. For this case, prey objects are those shown enclosed within the solid circle. After it begins its movement, the T shaped opaque barrier prevents the toad from seeing the prey. Solid lines to the left show the orientation of the toad's body axis, for several trials, during its pause at the fence end. Dashed lines are similar but for prey positioned within the dashed circle. These data make clear the toad's ability to 1) extract depth information from its visual world, 2) maintain a short-term memory of this depth information, and 3) integrate this memory with some notion of its own body movement. Reprinted by permission from Collett (1982).

We may note, with Ingle and Collett, that the full detour behavior exhibited here is quite complex: the animal does not simply orient towards the prey or the end of the barrier; rather, if it does not proceed directly toward the prey, it sidesteps around the barrier orienting in a way that depends upon the position of the target and the length of the sidestep. We postulate that each component of the behavior (sidestep, orient, snap, etc.) is governed by a specific control system called a *motor schema*. We then see detour behavior as an example of the coordination of motor schemas (Arbib, 1981), where the sidestepping schema acts to modulate the orienting schema. The full analysis of such motor schema coordination is beyond the scope of the present paper, but it is worth noting that Ingle (1982a) has offered us some clues as to the possible neural correlates of the various schemas: he finds that a lesion of the crossed-tectofugal pathway will remove orienting; lesion of the crossed-pretectofugal pathway will block sidestepping; while lesion of the uncrossed-tectofugal pathway will block snapping.

The strategy of modelling in this paper will be to first develop a simple one-dimensional model of detour behavior in terms of determining the initial target for the animal: namely, directly to the prey, or to one end or the other of the barrier. This preliminary model will be developed in Section 2. Then, after reviewing further data and ways of modelling depth discrimination in Section 3, we shall turn in Section 4 to a somewhat more sophisticated model where the choice of the direction in which to turn is augmented by the formation of an appropriate depth map to represent how far away the first target is in the given direction. Then, in Section 5, we look at a first model for generating the full spectrum of

information that should be available for a variety of motor schemas to not simply determine orientation and distance but to actually plan an initial sidestep around a barrier, the orienting movement at the end of this sidestep, and the final approach to the prey. It is our intention that, by considering a variety of models, we can create a space of alternatives in which the design of a rich set of neuroethological and neurophysiological experiments will be possible. Thus, Section 6 is devoted to a discussion of experiments suggested by the models and some of the open questions to be addressed by modellers.

2. The One-Dimensional Model

In the one-dimensional model, we represent the retinal input in terms of a map of neural firing rates indexed by the possible directions that the animal could turn in a horizontal plane. One of the first models of this kind (Didday; 1970, 1976) addressed the problem of the animal confronted with two or more fly-like stimuli, and offered a distributed neural network model of how the animal could come, in general, to snap at just one of these targets. This model was given mathematical form by Amari and Arbib (1977), and their primitive competition model is shown in Figure 2. Here, the 'tectum' is represented by an array of n cells, whose membrane potential at any time is u_i, with corresponding firing rate $f(u_i)$ – with the conversion of potential to firing rate shown by the graph of f at the bottom left hand of the figure. Each of these cells is driven by an input s_i which indicates the output of a preprocessing element corresponding to the likelihood that a prey is present in the corresponding portion of the visual field.

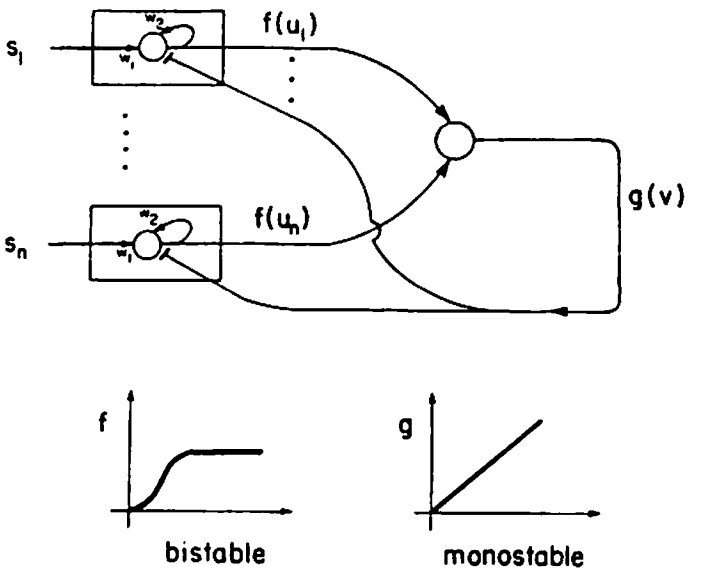

Fig. 2 -- Amari-Arbib Primitive Competition Model

This model selects the maximum stimulus from an input vector s by a non-linear, distributed, competitive process. Circles represent simulated neurons, arrow-headed connections to neurons are excitatory, and flat-ended connections are inhibitory. Input to the system is supplied by the vector S, w_1 and w_2 are excitatory weights, u is the vector of excitation levels in the input array of cells, and v is the excitation level in a cell that provides a global inhibitory feedback to the input cells. Functions f and g convert internal excitation to external firing rate. When properly tuned, the model will converge with only the element i, corresponding with the maximal input element s_i, above its firing threshold.

The cells are reexcited as shown, and also drive an inhibitory cell whose membrane potential v is converted into a firing rate g(v) which provides inhibition distributed to all the cells. Basically, with appropriately adjusted synaptic weights, we have that a cell will be able to continue its firing, thanks to its recurrent self excitation, so long as its initial stimulation is high enough to allow it to win out over the pooled inhibition of the other cells. Typical results of the mathematical analysis are that the synaptic weights can be set so that at most one element can be excited in an equilibrium, and that if all the u_i's are initially the same, and an element remains excited in the equilibrium, it is the one receiving the maximum stimulus. However, once the model has responded to one pattern of stimulation, the build up of inhibition will be such that the system exhibits *hysteresis* – it will not necessarily respond to the new maximal stimulus. However, a temporary change of threshold of all the units can be used to 'release' a 'blocked' response to a *new* maximal stimulus. It has been posited that this function is carried out in tectum by cells whose firing indicates a change in visual stimulation in their receptive fields – they are thus called newness cells.

Our first detour model (Epstein, 1979) is simply the Amari-Arbib model with a different input for prey and barrier stimuli. In Figure 3a (Epstein used a gerbil responding to sunflower seeds rather than a frog responding to flies or a toad responding to worms in his computer graphics) each prey-like stimulus is represented as a tectal input with a sharp peak at the tectal location corresponding to the position of the stimulus in the visual field, and with an exponential decay away from the peak. Note also that the size of the peak decreases with eccentricity. On

the other hand, as shown in Figure 3b, each segment of fence is represented by one trough of inhibition whose tectal extent is just slightly greater than the extent of the fence in the visual field. The sum of this excitation and inhibition when the three prey stimuli and the two barriers are combined is shown in Figure 3c, where the combined excitation of the two central stimuli is heavily lowered by the trough of the left barrier, but is still able to yield positive contributions at spatial locations just beyond the end of either barrier. Given the nature of the Amari-Arbib model of Figure 2, it then comes as no surprise that a computer simulation of the effect of such an input yields the situation shown at the top of Figure 3d in which it is the cells corresponding to the right-most end of that left-most barrier which first attain a sufficiently high level of firing to command the overt response of the animal as a move towards that end of the barrier. While our the next sections will refine this model in terms of the depth dimension, it seems worth exhibiting this sample run here because the logic of this model will constitute an essential subsystem of the model shown in Section 4.

Before closing this discussion we note one important feature of the data to be reviewed in the next section -- namely, that Ingle and Collett, in looking at the behavior of the animal confronted with prey and barrier, do not find a single unequivocal direction, but rather plot a histogram of directions of response over a number of trials. Collett (in a personal communication) reports that, except for very few animals that exhibit a strong directional preference, the histograms for multiple trials with single animals do not appear to differ significantly from those obtained across a population. Thus, it is important that a model yield not a single

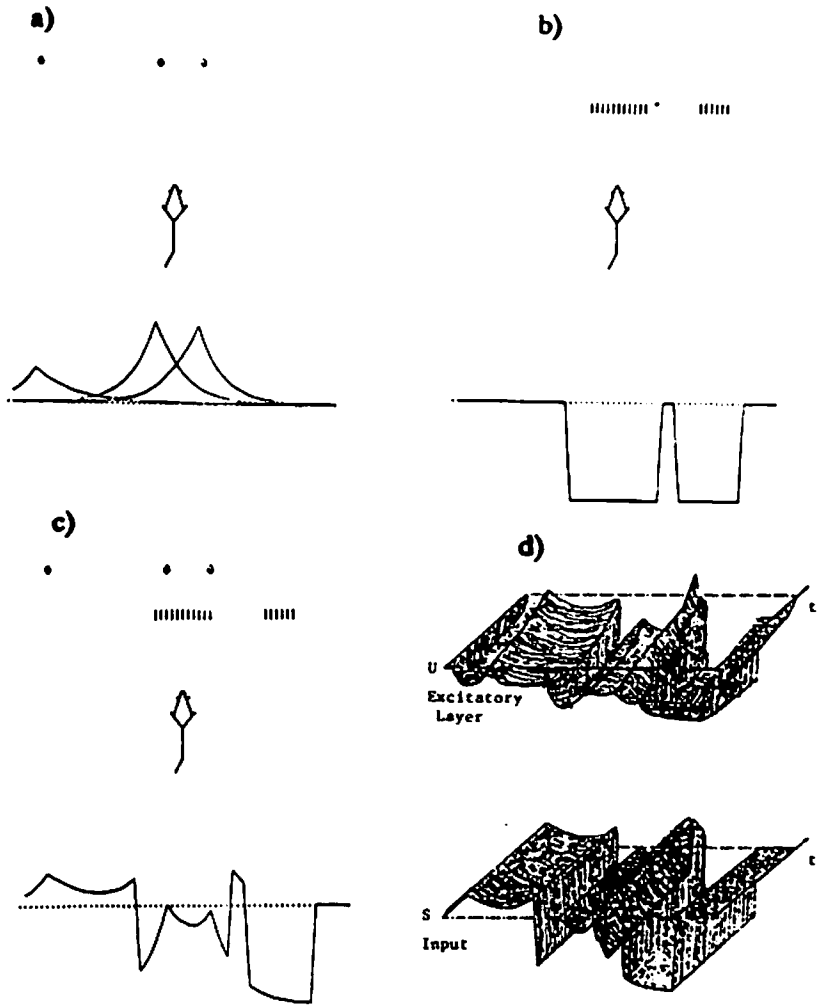

Fig. 3 -- Epstein's Prey Selection Model

In (a-c) the central object shows the position and orientation of a gerbil, the diamond-shaped icons represent food pellets, and vertically hatched regions represent barriers. The curves below the gerbil show spatially distributed patterns of excitation (regions above the dotted line), and inhibition (below the dotted line) elicited in the model by the configuration of pellets and barriers. In (a) the presence of three prey objects results in an overlapping pattern of excitation, whereas in (b) the barriers result in a trough of inhibition extending a small distance beyond each barrier end. The net effect of summing excitation due to pellets and inhibition due to barriers is shown in (c). The presence of inhibition leaves the maximally excited position to the right of the left fence. The curves traced in (d) show the time-course of the model in response to the stimulus pattern in (c). The time dimension t is drawn going into the paper, the horizontal axis represents the spatial dimension and the vertical axis the level of excitation. The curve of input vector S (bottom) simply shows the stimulus pattern of (c) held constant as time advances. The curve of excitation level U (top) shows that the model eventually converges with all orientations suppressed except for the one corresponding with the initial maximal input. According to the assumptions of the model, this triggers a turn to the right edge of the left barrier.

unequivocal response, but rather that it be capable of yielding a histogram of preferred directions. The first strategy that suggests itself is to replace deterministic neurons by stochastic neurons whose output is driven by a noise term as well as by the other inputs. A second strategy, and an important one for many classes of non-linear models, is to vary the initial conditions while keeping the elements of the models deterministic. However, a third strategy will be followed here, and that is to identify an explicit model parameter which is likely to be subject to significant variation due to motivational state and immediate experience of the animal, and whose variation will readily affect the model's convergence characteristics. For example, in Section 4 we show how such a variation in the spread of excitation due to prey-like stimuli can have significant effects on the behavior of a model of orientation behavior.

3. Introducing the Depth Dimension

This section briefly reviews data indicating the need to take the depth dimension into account in any model of detour behavior in the toad. After that, we will sketch the general setting for our models of Sections 4 and 5, and close the section by briefly comparing two recent models of depth discrimination.

Figure 4 (Collett, 1982) shows a number of experiments on detour behavior. In each case the solid square with tail indicates the initial position of the toad, a row of dots indicates the position of a barrier, and the rectangle with squiggles represents the position of the worm. Arrows are labelled with percentages which show how frequently the indicated directions were chosen by the animal over a

large number of trials. Figure 4a shows that the animal will prefer to detour around an uninterrupted barrier, while Figure 4b shows that the animal will prefer to go through a gap rather than detour. It is interesting to contrast Figure 4c with Figure 4a. In Figure 4c there is an uninterrupted fence at the same position relative to toad and worm as in 4a, but now there is the fence with a gap as in Figure 4b in front. In this case, the animal discounts the rear fence by choosing to go through the gap more than half the time, even though it would have detoured around the rear fence 3/4 of the time in the situation shown in Figure 4a. Thus, it would seem that, to a first approximation, the response of the animal is a weighted sum of its responses to the individual fences, with the effectiveness of a fence in the sum declining with distance. Figure 4d shows that the animal's tendency to detour is strong when both the near and far fences are uninterrupted; while Figure 4e shows that with a large gap in the front fence, the toad overwhelmingly chooses to go through the gap even when, as in this case, there are side fences joining the front and rear fences so that the animal's behavior is in fact to enter a cage. Such results lend weight to the search for a model which does take the depth dimension into account, but which is not highly cognitive in a sense in which the animal would be posited to use representations of such high-level constructs as one fence vs. two, or a gap vs. a cage.

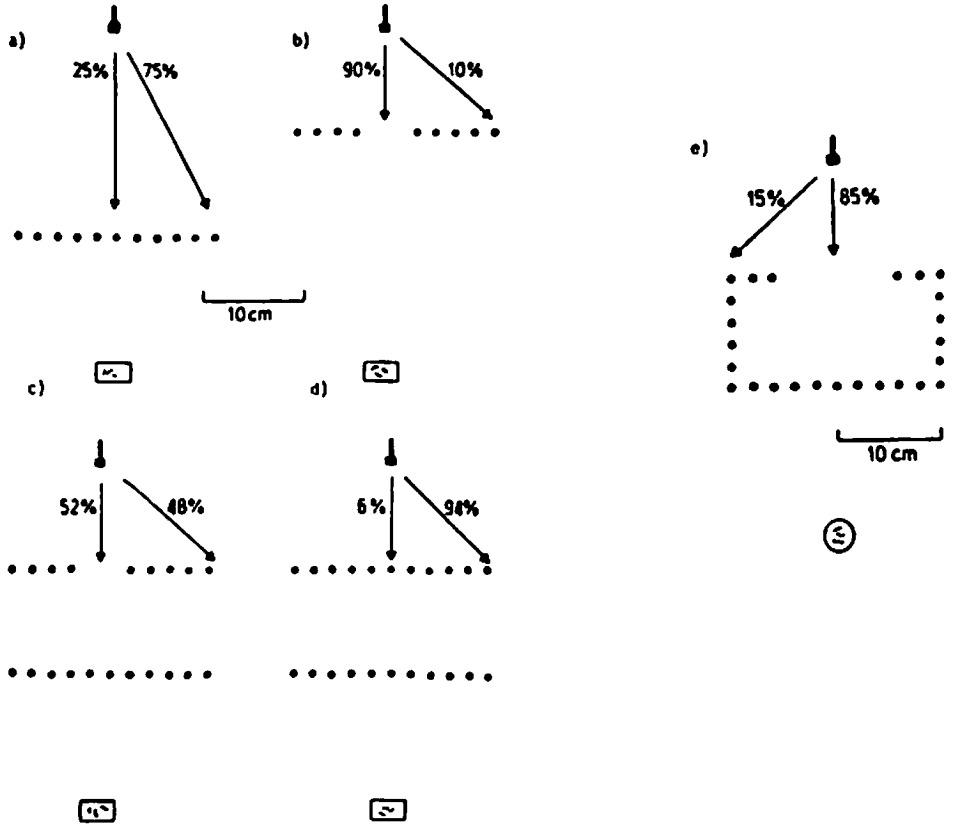

Fig. 4 – Prey/Barrier Experiments

Histograms of the initial orientation response of a toad presented with various prey/barrier configurations. Configurations are shown in top-view. Rows of dots represent paling fence barriers, large circles indicate prey position, and the inverted T's represent the position and orientation of a toad. Distances are to the scale shown in the diagram. Percentages indicate the number of trials on which the animals elected to head directly towards the prey versus the number on which they elected to detour around either of the fence ends. Reprinted by permission from Collett (1982).

Figure 5 superimposes two possible coordinate systems for representing the ground plane in front of a frog or toad. This figure also introduces the graphical notation to be used to describe the visual scenes which form the input to the models of Sections 4 and 5. The T shaped object at the bottom of the figure represents the animal, with the disks at the ends of the crossbar indicating its eye positions. The small disks within the grid area represent fenceposts and the solid rectangle a prey object. The 40 cm. by 40 cm. ground plane is divided into a cartesian grid with an interval size of 10 cm. The radial coordinate system overlaid upon this grid is centered on the midpoint between the two eyes. The radial lines of this system are placed at intervals of 7-1/2 degrees. The curved lines are lines of constant visual disparity, spaced apart by a constant disparity increment.

We posit that neurons may be more appropriately indexed by the radial system than by the rectangular coordinates. The use of an angular measure is clearly motivated by the way in which an image is projected onto the retinal surface. Also, since disparity cues, like other depth cues, are more acute closer to the animal, the curves are longer and further apart with increasing radial distance from the animal. Thus, they have a general appeal as a system for the representation of depth and, we would posit, represent regions which have approximately the same density of neural representatives. Note, however, that Figure 5 simply represents the ground plane of the animal, and not the full visual field. One structure which could support the full representation is a mapping of the whole ground plane onto a linear strip of cells in the brain, with each small region in that strip corresponding to a single angular direction, but a full range of depth, with the

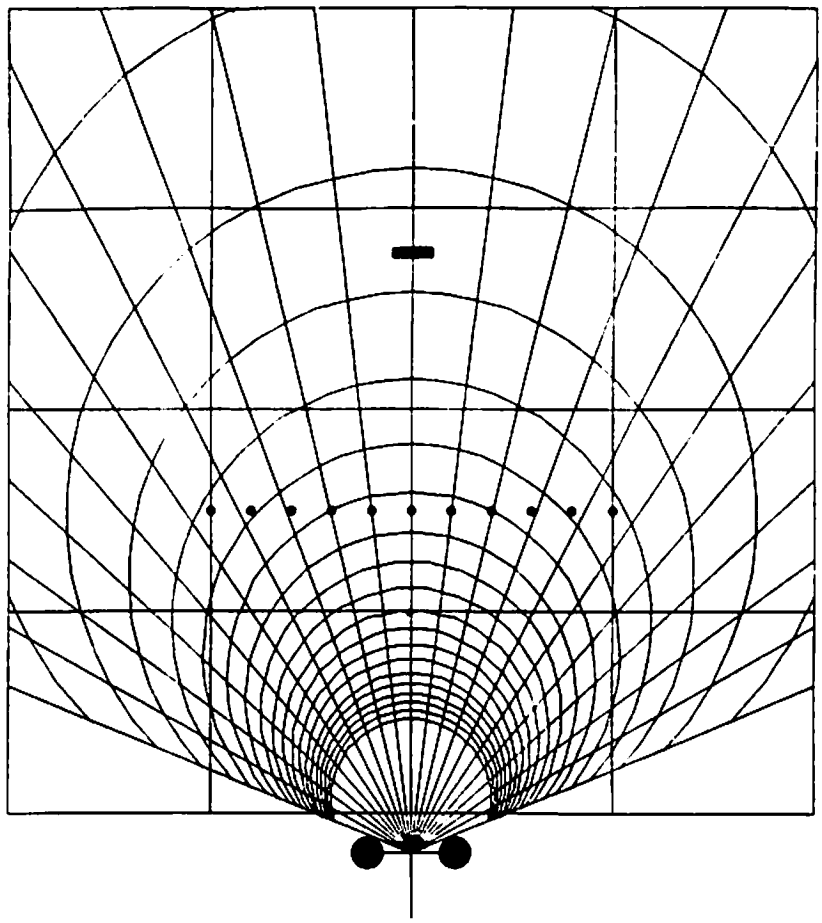

Fig. 5 -- Coordinate Systems Used for Orientation Models

Cartesian and radial coordinate systems used in the models. The area shown represents a 40 cm. by 40 cm. square in top-view. The cross-like icon at the bottom of the figure represents a toad with eyes at the positions of the dark filled circles. The darkened rectangle in the upper-central part of the grid represents a prey, and the dots across the lower-central portion represent the posts of a paling fence. Squares of the cartesian grid are 10 cm. on a side. In the radial system the radial lines are at equal angular increments from the toad's midline, and arcs are lines of constant disparity spaced at equal increments of disparity. The spacing of the equi-disparity arcs illustrates the decrease of depth acuity with increasing distance from the animal.

proportion of cells representing nearer depths much greater than the proportion of cells representing further depths. In summary, we represent the ground plane by neurons indexed by an orientation coordinate θ, and a discrete depth zone coordinate d, but do not posit that θ and d also function as the coordinates for a two-dimensional array of neurons.

The general scheme of the detour model is then as shown in Figure 6. The visual input to the retinas provides two maps based on the θ coordinate which can be further processed to yield depth mappings. We have made the assumption that the barriers are recognized by one population of cells and processed for depth separately from worm-like stimuli which are represented by a separate depth mapping. This assumption is supported by the work of Ingle (1977) and of Ewert (1976) who demonstrated the likelihood that processing of prey stimuli is localized to the tectum whereas contraindicative stimuli are processed in the pretectal region. By this assumption it is possible for these two mappings, indexed by the (θ,d) coordinates, to be separately convolved – the barrier depth mapping B being convolved with a kernel I which assigns inhibitory weight to barriers, and the worm depth mapping W being convolved with a kernel E which assigns an excitatory weight to the prey. The resulting sum $B*I + W*E$ then provides the input for the target selector and the output of this target selector can be combined with the barrier and worm depth maps to provide the necessary input to coordinated motor schemas for the motor output for snapping, sidestepping, orienting, jumping, etc. We shall provide two different instantiations of this general model scheme in Sections 4 and 5. The rest of this section briefly describes recent work on modelling depth perception.

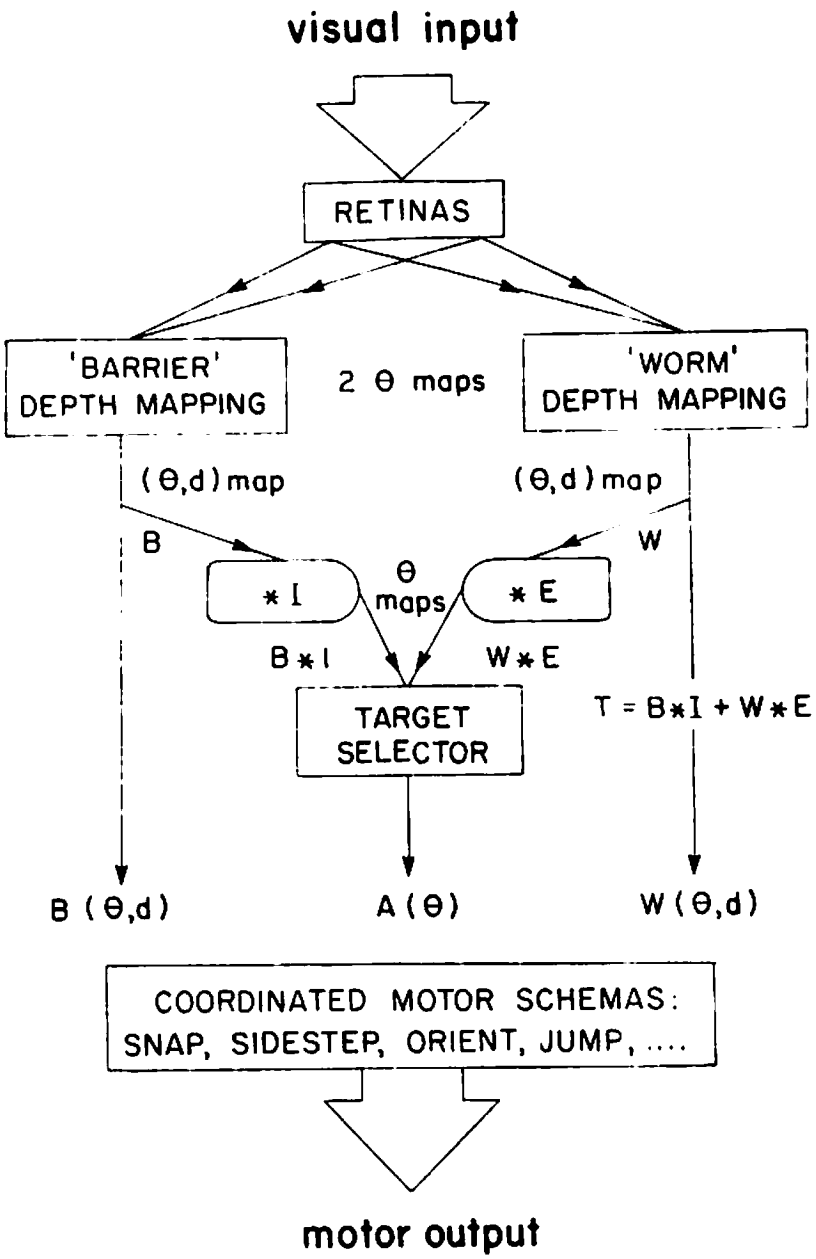

Fig. 6 – Conceptual Schematic of Visual/Motor Pathway

This diagram depicts our view of a general scheme by which visual input could be processed to produce motor output. This scheme is based on assumptions that 1) separate depth maps are maintained for prey and barrier stimuli, 2) the direction for an orientation turn is obtained by combining information from these two maps, and 3) information on preferred orientation and depth of prey and barriers is simultaneously available to the various motor schemas. The motor schemas are, in turn, capable of integrating this information with information about current body position to produce a coordinated motor-output.

Recent Models of Depth Perception

It is well known (Julesz, 1971) that the input to a single eye at a given time does not in and of itself convey depth information. Among possible mechanisms for extracting depth information are lens accommodation, binocular disparity matching, and optic flow from the change in input to a single eye over time. Recent evidence indicates that toads must integrate information from at least two of these sources when determining the depth of prey.

On the one hand, Ingle (1976) showed that monocularly blind frogs will snap accurately within the intact monocular field, and in the ipsilateral portion of the normal binocular field. He suspected that lens accommodation was the source of these monocular depth estimates, since estimates were systematically distorted within the contralateral binocular field in a way which might be predicted by the decreasing resolving power of the lens in its periphery. The conclusion from these observations is that monocular depth cues are sufficient for frogs to determine depth of prey, and that lens accommodation is the probable cue source. These conclusions have since been confirmed by Collett (1977) and Jordan et al. (1980). On the other hand, by fitting toads with prisms and testing their prey catching abilities, Collett (1977) was able to show that binocularity dominates the depth discrimination process in normal binocular toads. His experimental data suggest a 94% contribution from binocular cues and only a 6% contribution from accommodation. These results taken together indicate that binocular cues dominate when they are available but monocular cues are sufficient in the absence of binocular cues.

This evidence for the use of multiple depth cues led us (House; 1982, 1984) to develop a model which extended earlier depth perception models by Dev (1975) and Amari and Arbib (1977). We call this model the Cue Interaction Model. Its overall structure is depicted in Figure 7. It uses both accommodative and disparity-matching cues to guide a cooperative-competitive process that segments a visual scene into depth regions. Further, it is possible to tune the model so that depth cues from binocularity dominate, while monocualar accommodative cues remain sufficient to determine depth in the absence of binocular cues. The model produces a complete depth map of the visual field, and therefore addresses the problem of collecting the kind of depth information necessary for barrier navigation (this task is explored in the next two sections). In computing the binocular disparities necessary to produce these maps, however, the model relies upon binocular visual input to a single neural surface.

More recently, Collett and Udin (1983) used lesion experiments to demonstrate that, at least for the more limited problem of unobstructed prey catching, toads are able to make accurate binocularly-based depth estimates even after the major cross-brain binocular relay (nucleus isthmi) has been severed. To explain their results, Collett and Udin postulated that the toad may use a neurally-implemented triangulation process to localize prey, rather than a process based on disparity matching. This postulate suggests a depth resolving system that does not attempt to produce a complete depth map but instead selects a single point and locates that point in space (i.e., the position of a prey).

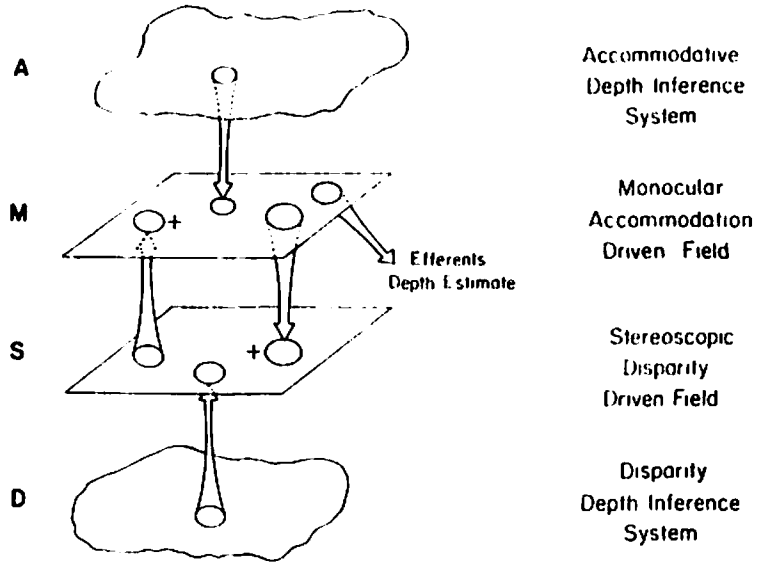

Fig. 7 – Schematic View of the Connectivity of the Cue Interaction Depth Model The various layers of the model and their interconnections are shown. Layer A represents an inference system that provides monocular depth cues from lens accommodation, and layer D represents an inference system that provides binocular cues from disparity matching. Layers M and S represent spatially organized fields over which two depth-mapping processes operate. Arrows from layers A and D to these fields indicate that field M receives only monocular depth cues, and field S receives only binocular cues. The ovals and arrows between fields M and S indicate mutual excitatory interconnections that map each local region (oval) of one field onto the corresponding local region of the other field. By means of these interconnections, points of high excitation in one field provide additional excitation to corresponding points in the other field. Competition among depth estimates within each field assures that points excited in only one field will have little chance to sustain this excitation when there are other points receiving stimulation in both fields.

Our most recent depth modeling efforts have been directed at exploring the postulate of Collett and Udin, while still incorporating the use of multiple depth cues. These efforts lead to the development of the Prey Localization Model (House, 1984). This model is summarized in Figure 8. It uses pattern recognizers and prey selectors on each side of the brain to select and identify the position of a prey target on each eye. The right and left eye positions are used to compute a depth which is used, in turn, to adjust lens focus. If the selected points on the two eyes correspond with the same point in space then the depth estimate will be accurate and the object will be brought into clearer focus. This effectively locks the system onto the object. If the points do not correspond then the computed depth will be incorrect, and the resulting lens adjustment will usually serve to bring one of the objects into better focus while simultaneously degrading the focus of the other object. Consequently, the system will tend to choose one of the objects over the other and will eventually correctly locate this object.

Neither of our depth models can, by itself, fully explain the complete range of data on the depth resolving system of toads. The Cue Interaction Model successfully integrates binocular and accommodation cues in a way which allows it to replicate behavioral data. However, it relies on a neural connectivity that does not appear to be necessary for binocular depth perception. The Prey Localization Model successfully addresses the lesion data, and integrates both depth cue sources. However, it is not capable of operating in a purely monocular mode. Further, this model does not allow us to address as broad a range of visual data as does the first model. In particular, it locates only a single point in space and is, therefore, not well suited to locating barrier-like objects. It may well be that instead of there

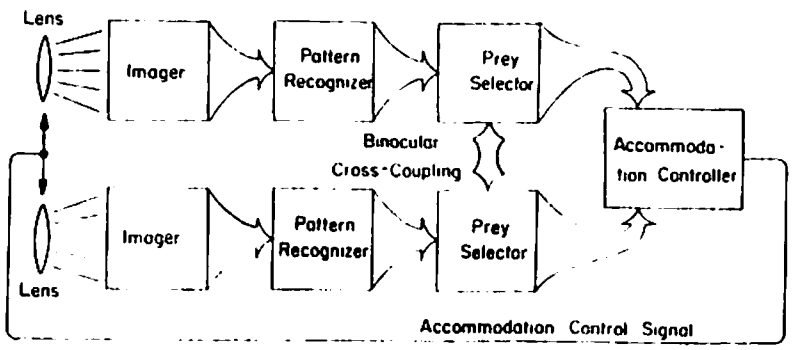

Fig. 8 – Prey Localization Model Schematic

The functional components of the model and their interconnections are shown. Lenses are coupled so that they are accommodated to the same depth. Imagers produce visuotopically mapped output signals whose intensity is proportional to the crispness-of-focus at each image point. Pattern recognizers produce visuotopically mapped output signals that are strongest wherever the image most closely corresponds to the recognizer's matching criteria. Prey selectors take their input from the recognizers and from cross-coupled connections with each other. Their outputs are highly selective, giving a high weight to points receiving the maximum input stimulation and suppressing all others. Since the prey selectors take their input both from the pattern recognizers and from cross-coupling they are biased in favor of points receiving strong stimulation on both sides of the binocular system. The accommodation controller converts the weighted image coordinates from both prey selectors into an estimate of depth. It then uses this calculated depth to adjust the lenses.

being a single general depth-perception mechanism, that we have here a case of various neural strategies functioning either cooperatively or alternatively to cope with the vast array of visuo-motor tasks required of the freely functioning animal. Elsewhere (House, 1984) we describe one way in which both of the processes outlined in our models might be integrated in the brain of the toad. Figure 9 shows our proposal for how these two processes may be distributed in the toad's brain. Caine and Gruberg [1985] provide support for the anatomical separation of Figure 9, but their results are in flat contradiction to those of Collett and Udin, posing a clear challenge for both future theory and future experiment. They found that frogs with lesions of n. isthmi failed to respond to either threat or prey stimuli presented in the corresponding region of the visual field (contradicting Collett and Udin); while they exhibited normal barrier-avoidance and optokinetic nystagmus in all areas of the visual field (consistent with the scheme of Figure 9). They conclude that the behavioral deficit seems to be 'visual' and not 'motor', and appears to be identical to that induced by unilateral tectal aspiration.

In developing the barrier negotiation models which are outlined in the following two sections, we have thus made the assumption that toads are able to infer the depth of barriers and prey simultaneously and that this information is either determined by different neural substrates or is at least separable by object category.

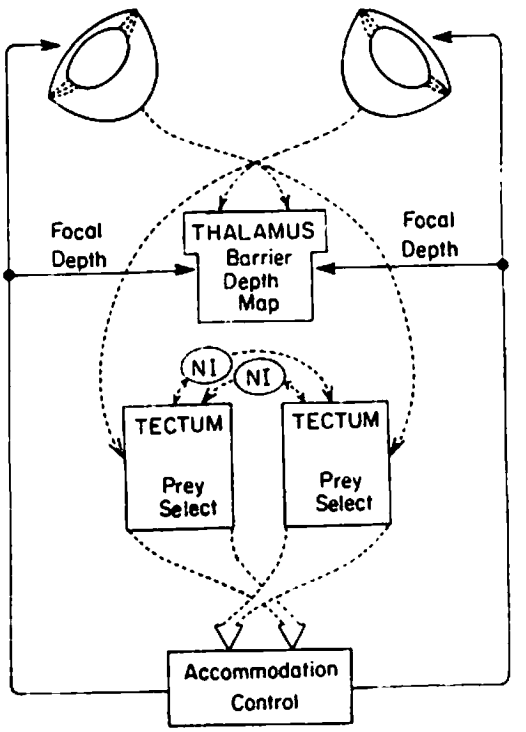

Fig. 9 – Possible Anatomical Distribution of the Integrated Depth Perception System This diagram shows how both depth mapping of barrier surfaces and localization of prey may be distributed in the nervous system of frogs and toads. Eyes are represented at the top of the figure, and internal brain regions are indicated by labeled rectangles. Dashed arrows depict information inflow, and solid lines represent outflow. The thalamus receives overlapping projections from both eyes as well as signals indicating the current lens accommodative state. These inputs would allow the development of a depth map of visual space using a mechanism similar to that outlined in the 'cue interaction model.' Each tectal lobe receives only a monocular projection from the contralateral eye, but ipsilateral information is available from tecto-tectal relays through the nucleus isthmi (NI). These inputs provide tectal prey selectors with the information necessary to localize a single prey. Prey selector output projects to the accommodation controller.

4. A Model for Choosing Orientations

This section presents our first model of detour behavior to take depth into account, specializing the general scheme of Figure 6 in the manner shown in Figure 10a. Here, the depth map for prey is convolved with the excitatory mask shown in Figure 10b and the depth map for the barrier is convolved with the inhibitory mask shown in 10c to yield two two-dimensional arrays whose sum is shown as array E in Figure 10a. The shapes of the two masks were chosen to take into account the way in which toads, when confronted with a 'prey behind barrier' configuration, make the choice between turning around the barrier or proceeding directly towards the prey. Collett (1982b) reported that what governed the path selection was (1) the distance of the worm from the fence, and (2) the absolute length of the fence. Within a 20 to 30 cm. distance from the toad, neither the distance of the toad from the fence nor the visual angle subtended by the fence seemed to be important. Thus, the mask for barrier edges (fence posts) was chosen to project behind the edge at a constant maximum height after an initial rise to that maximum, i.e. there is a short distance behind the edge in which there is little inhibition, after which inhibition is equally strong at all distances. The mask for prey objects projects very broadly in a lateral direction and somewhat less broadly in the forward direction. The net result is that with a prey object significantly far behind a barrier the barrier projection substantially reduces the prey projection except beyond the barrier ends. For prey close to the barrier the prey projection is not significantly reduced and is thus strongest directly in front of the prey. To approximate the 'size constancy' exhibited by actual animals the effects of the

non-cartesian coordinate system are partially counteracted by decreasing the spread effect of the masks by a linear factor with increasing distance from the toad.

The input depth maps D_b and D_p are assumed to be cleanly segmented as to depth, so that there is at most one computed depth for barrier and one computed depth for prey in each visual direction. This is not the case in E, which represents the superposition of the convolutions applied to these two arrays. We thus subject E to two independent processes in the present model. In the left-hand path of Figure 10a, we integrate the total excitation along each visual direction, to provide a one-dimensional map which is then fed to an orientation selector model which will extract the orientation θ of maximal total excitation. Thus, this portion of the model is an extension of the one-dimensional model presented in Section 2. However, the present model also subjects the map E to a further process of depth segmentation. Thus, when the orientation selector returns an angle through which the animal is to turn, the motor schemas can also consult the depth segmentation model to provide the depth at which the target at orientation θ is to be found. Note that the target being considered now may not correspond to the initial prey stimulus. Instead, it represents the point in space to which motor activity will be directed. If this point corresponds to the prey location the object is achieved. Otherwise, we suggest that further processing will ensue upon reaching this target.

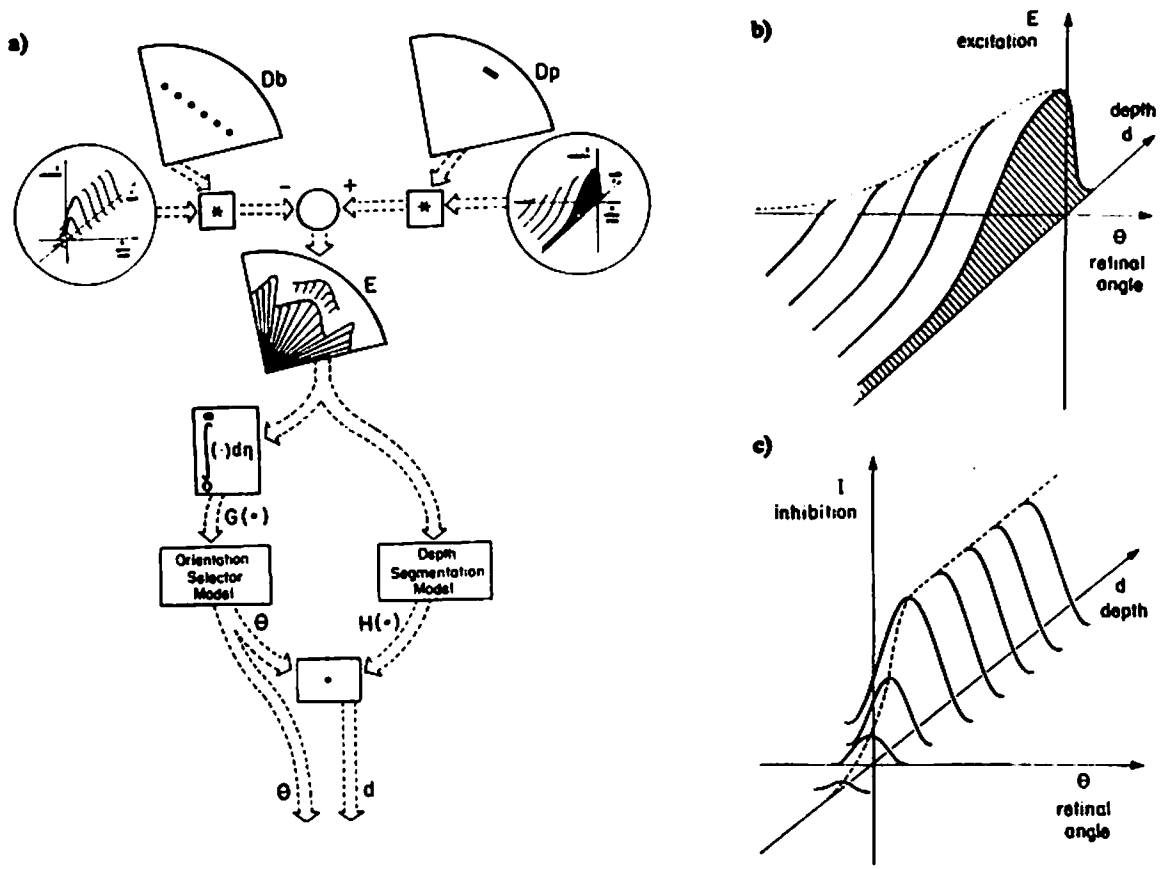

Fig. 10 – Orientation Model, Implementation Schematic

The general model of Fig. 6 is shown here in a specific implementation that is specialized to the barrier negotiation problem. (a) shows the information flow and indicates the operations performed. Here, D_b represents the barrier depth mapping, and D_p the prey depth mapping. (b) and (c) show the details of the spread functions which are convolved with the prey and barrier depth-maps to produce selection surface E. Surface E may have multiple peaks at a given visual direction, so E is resegmented in depth in order to produce the vector H which encodes a single depth target for each angular orientation. The orientation of the selected target is provided by a Primitive Amari-Arbib Model which takes as its input the vector G obtained by integrating, for each orientation angle, total excitation along the depth dimension in surface E. The selected orientation angle θ is then used to index H to yield depth d.

Figure 11 shows the operation of this model on the single worm behind a single barrier configuration pictured in Figure 11a. The length of the arrow with orientation θ at the base of 11b corresponds to the total excitation $G(\theta)$ which is provided as input to the orientation selector model for that θ. The array of squares and ovals represents the input E to the depth segmentation model, with ovals corresponding to inhibition and squares corresponding to excitation. The level of intensity of either excitation or inhibition is encoded by the size of the corresponding symbol. As we see in 11c, the direction chosen by the orientation selector model in this case is that of the left-hand end of the barrier, and the squares indicate that the depth returned by the depth segmentation model does indeed correspond to the end of the barrier.

Figure 12 shows the ability of the model to replicate some of Collett's behavioral data. Figure 12a depicts a fence and worm configuration identical to that of Figure 11 except for a gap in the center of the fence. To the left is the model input and to the right is the converged state of the model. Here we see that the preferred direction is now straight ahead, and that depth information is provided for the edges of the gap and for the worm. Figure 12b shows data for the case of a solid fence moved back to a position near to the worm. Here the preferred direction is also straight ahead. In Figure 12c we have the net result of placing a fence containing a gap in front of a fence near to the worm. Again, the directional preference is straight ahead towards the worm. Finally, the cage of Figure 12d gives similar results.

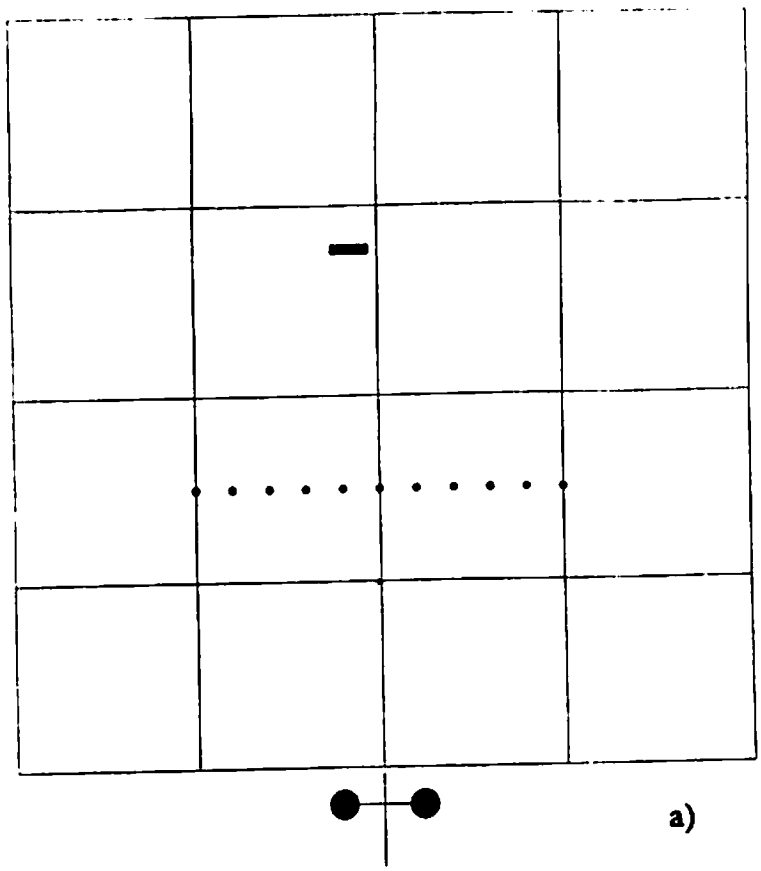

a)

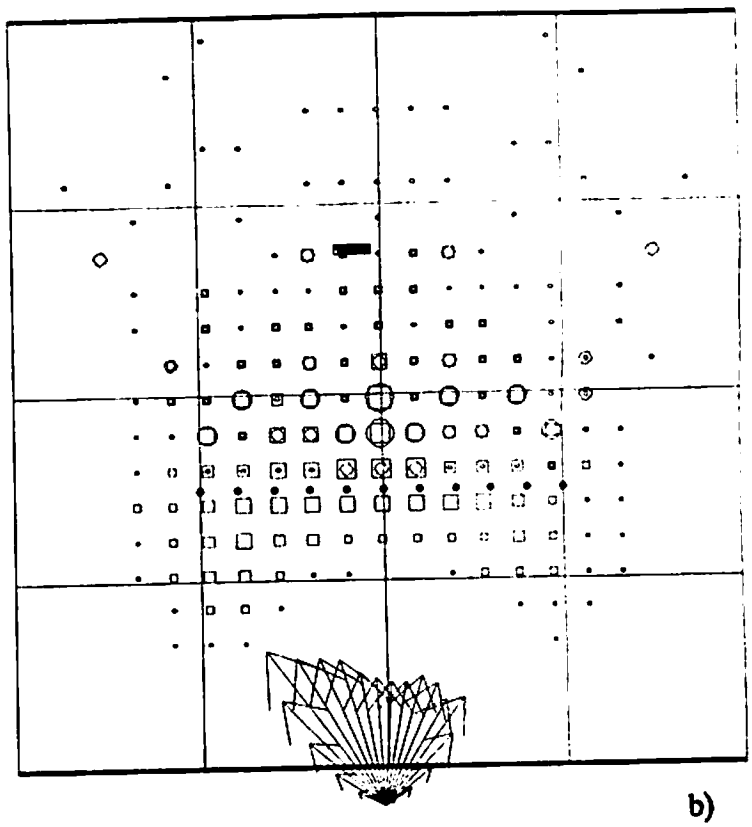

b)

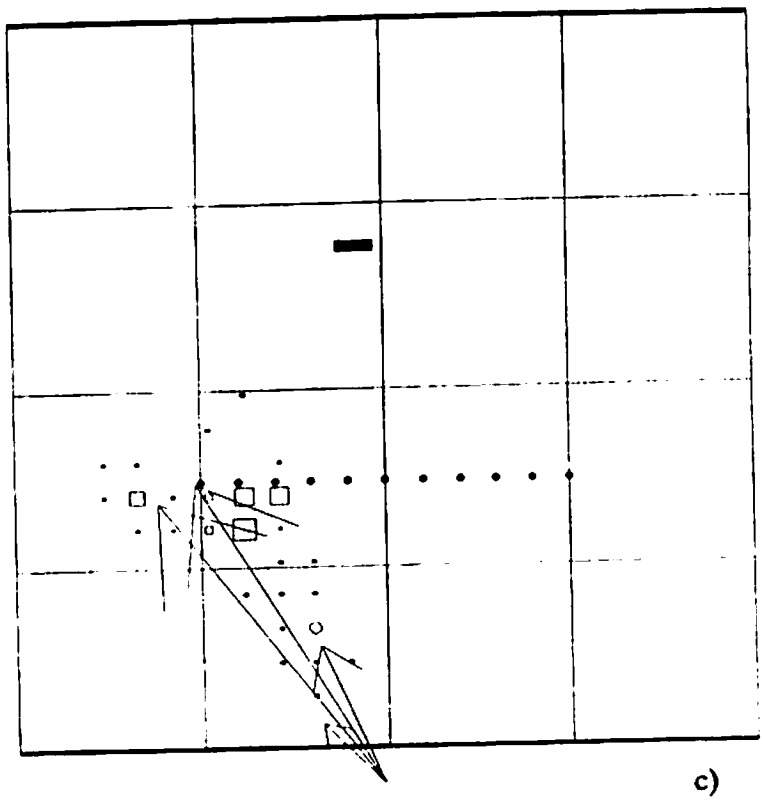

c)

Fig. 11 – Orientation Model, Test Case

(a) The scene used as input to the model, showing a single prey behind an unbroken fence. (b) The selection surface E is shown superimposed upon the original scene. Square blocks indicate areas of excitation due to spread of the prey stimulus. Ovals indicate inhibition from fence-posts. Strength of excitation or inhibition is indicated by the size of the corresponding symbol. The arrows indicate the visual direction and strength of the elements of the vector G which provides the input to the orientation selector. (c) After nearing equilibrium the model has selected a single orientation preference to the left end of the fence, and a localized set of preferred depths (indicated by the squares near the left fence end).

In order to address the variable orientation preference indicated by Collett's histograms (Figure 4) we present the set of experiments shown in Figure 13. These 9 runs were made with three different distances of a solid fence from a single worm. For each fence distance three choices of the prey spread function were made. The minimum spread necessary to cause selection of a fence end for the farthest fence distance was chosen as the base spread. The figures show model input, with the large circle centered on the direction and distance selected by the model when run against this input. The left-hand column of figures was made with a spread 33 percent greater than this amount, the central column with the base spread, and the right-hand column with a spread 33 percent less than the base value. We see here that the model shifts preference between the fence ends and the fence middle depending upon the extent of spread. In no case does the model converge upon an orientation other than towards a fence end or directly towards the worm. The variation in the sensitivity of orientation preference as a function of the distance of the fence from the prey is qualitatively consistent with behavioral results previously demonstrated by Collett (1982b). Further research, however, needs to be done to test the quantitative adequacy of the model.

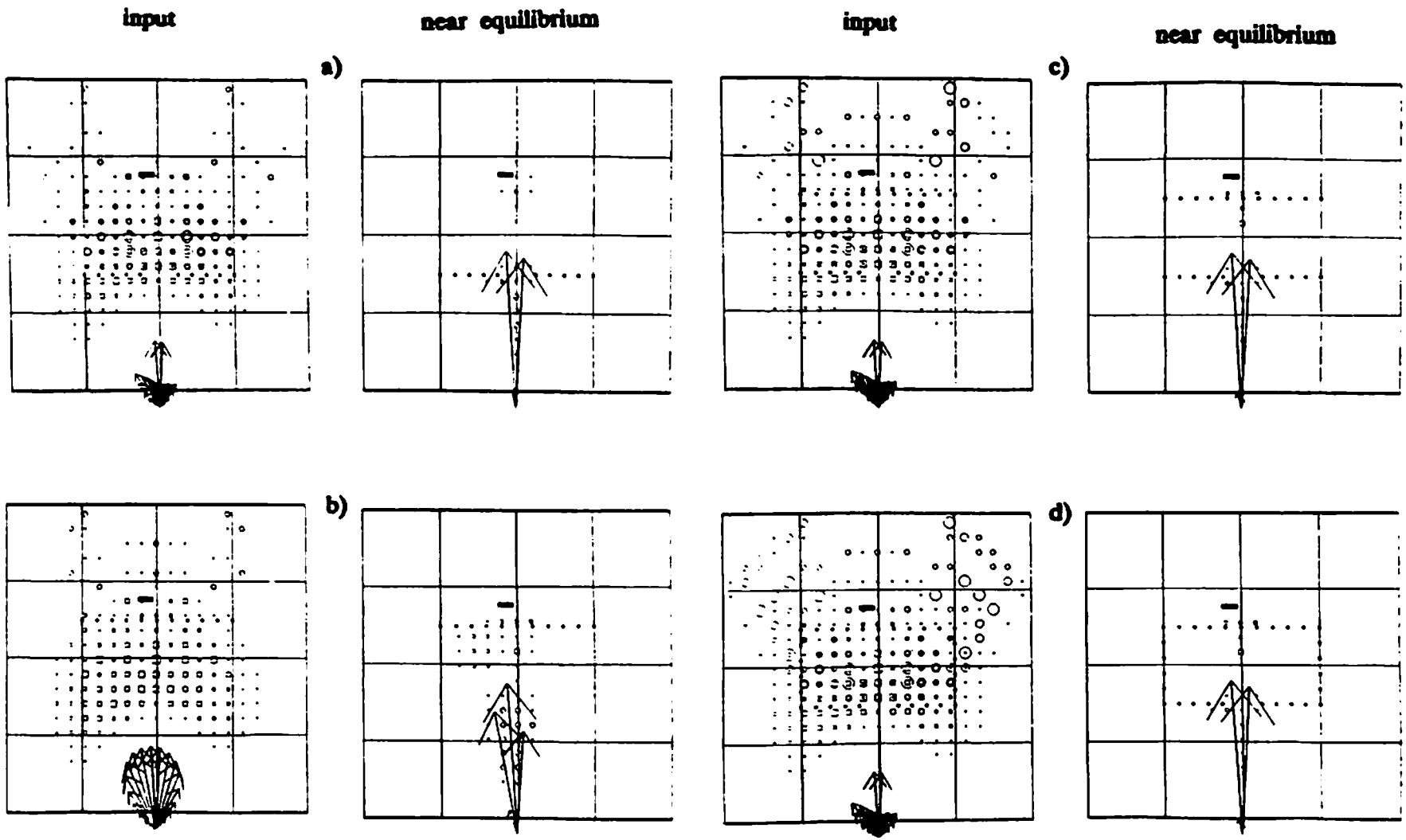
input
near equilibrium
input
near equilibrium
a)
c)
b)
d)

Fig. 12 – Orientation Model, Comparison with Behavioral Experiments
The selection surface and equilibrium state for several configurations used in behavioral studies. (a) Fence with gap. (b) Solid fence close to prey. (c) Fence with gap in front of solid fence. (d) Cage. The model results are consistent with behavioral results (compare with Figure 4).

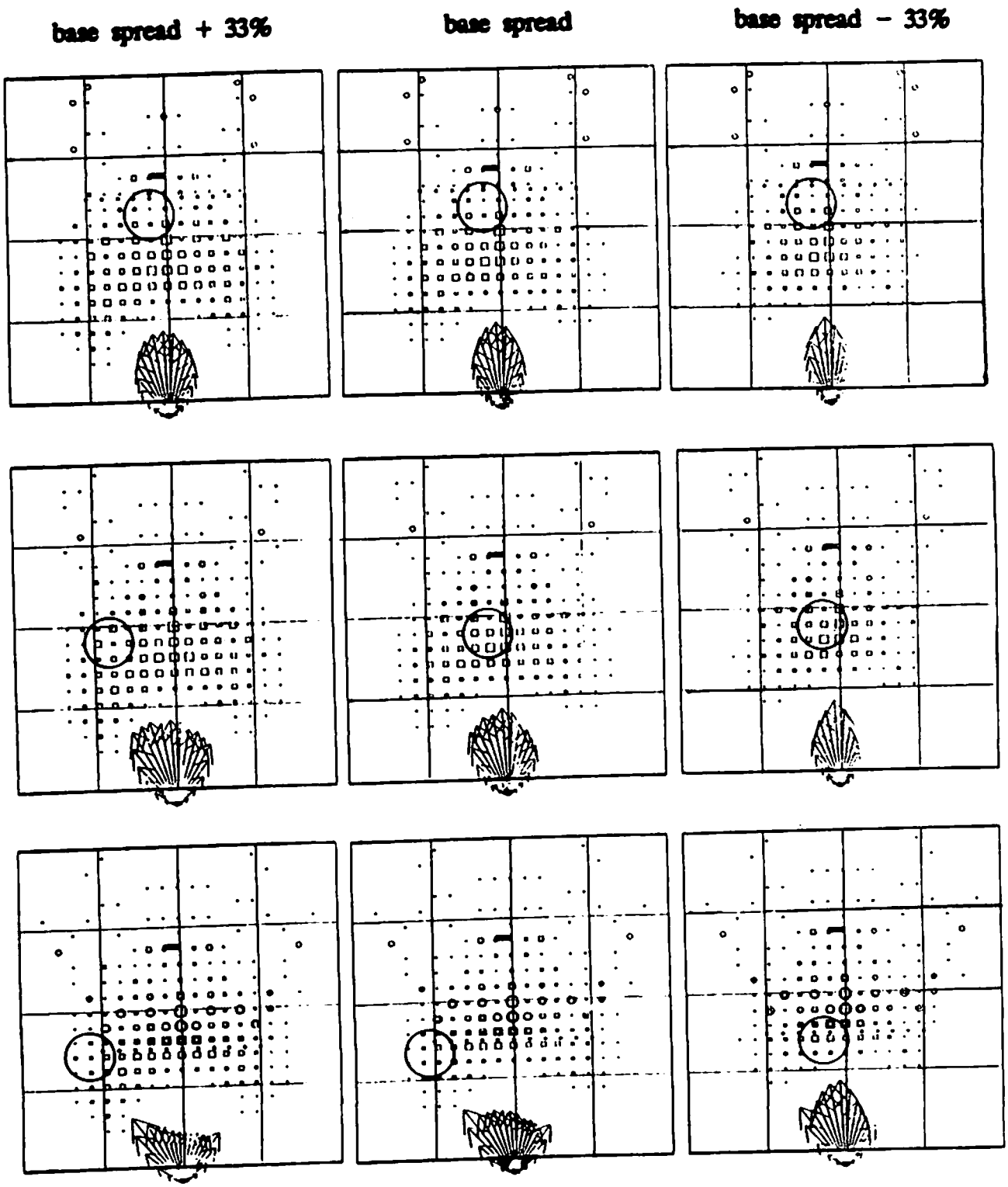
base spread + 33%
base spread
base spread − 33%

Fig. 13 – Model Performance for Various Fence Distances and Spread Parameters
The nine trials shown here were made with three distances of the fence from the prey and, for each distance, three settings of the prey attractant spread parameter. The images shown are the model input for each configuration, with the approximate spatial target selected by the model indicated by a large circle. The 'base spread' used in the central images was that which just caused the model to select a fence end for the farthest fence distance. The model's choice of fence end vs. direct approach to prey is highly sensitive to this parameter, thus suggesting a way in which the variation in actual animal behavior might be explained.

5. A Model for Planning Paths

Both the preliminary model of Section 2, and the depth-based model of Section 4 serve simply to choose the direction and, in the latter model, the depth of the target for the animal's first move. It is not clear from such a model how the animal would determine whether that target is the target for a sidestep as in detouring around a barrier, or for a snap, as in direct approach to the prey, nor is it clear how such a model would explain how the animal has in its brain the necessary information to determine the subsequent orientation following a sidestep if that is what first occurs. In the present section, then, we turn from models based on the selection of a single target to models which suggest how the brain might go about planning overall paths of action which would require the coordination of several motor schemas. We present the two models of Sections 4 and 5 side by side because we believe that at this preliminary stage of the search for the neural substrates of detour behavior, it is premature to focus on a single model. It is hoped that the contrast between these models will serve to stimulate the design of new behavioral and physiological experiments. We also stress that the models are not tightly constrained, in that they do not attempt to specify what particular neurons are doing in the posited behaviors. Rather, they represent processing schemes which could plausibly be carried out in neural structures, and thus represent postulates that there are populations of neurons which carry out the indicated operations. We pose it as an important challenge to lesion studies in collaboration with studies in neuroethology, neurophysiology and neuroanatomy to determine whether indeed there are neural structures which do perform these operations, and

then to determine whether the posited functional interactions do indeed take place between the layers thus identified. We expect that the refinement of our models will go hand in hand with the development of further data of this kind, and that theory and experiment will provide each other with important stimulation.

The depth selection portion of the model in Figure 10 had an excitatory field whose neurons were specified by two coordinates, one for angular direction, and one for depth or disparity. We then postulated that the activity of the neuron with coordinates (θ,d) was to be seen as a measure of confidence that there was indeed a feature in the external world at the corresponding position in the visual field. The function of the model was to converge upon a configuration in which only one depth was given a high confidence level for each visual direction. In the present model, we associate with each coordinate not a single number but a vector, and this vector is to indicate the preferred direction of motion of the animal were it to follow a path through the corresponding point. For conceptual simplicity, and not because of any change in thinking about what internal representation is most likely, the coordinate system used in this model is the Cartesian (x,y) system. Our task with this model will be twofold: to specify how the vector field is generated; and to specify how the vector field is processed to determine the appropriate parameters for the coordinated activation of motor schemas. In the technical jargon of differential geometry, then, the neural surface corresponds to a manifold representing space in some internal coordinate system, while the firing of a group of neurons associated with a particular coordinate is to represent the vectors of a tangent field, or flow. The question is how those local vectors are to be integrated to determine overall trajectory for the animal.

At the current stage of our research, we would wish to suggest that the model that follows is meant to indicate a style, rather than to be seen as a fully articulated hypothesis about the nature of the vector fields that could be represented in the visuomotor system of the frog or toad -- or the gerbil. Our first choice is shown in Figure 14. Figure 14a suggests that a single prey will set up an attractant field, in which from every point in the animal's representation of space there is an arrow suggesting a choice of movement toward the prey, with the length of the vector (the strength of choice for a movement in the given direction) being the greater, the closer is the point to the prey. Figure 14b shows that we have associated a repellant field with a single fencepost, with the strength of the field contributing mostly to the determination of a lateral movement relative to the position of the fencepost from the viewpoint of the animal. Finally, in Figure 14c we have the animal's representation of itself within this field. This representation simply consists of a set of vectors radiating out in all directions from the animal's current position with a decay similar to that for the prey field. Figure 15 shows the various effects obtained by summing the vectors for each point of the manifold. In Figure 15a we have the bug attractant field in interaction with the animal's self representation. In Figure 15b we see the summed effect of the fenceposts corresponding to a field which repels from the fence as a whole but with especially strong lateral flow at the edges of the barrier. Finally, in 15c we have the overall net field set up by a scene containing a single worm behind a fence.

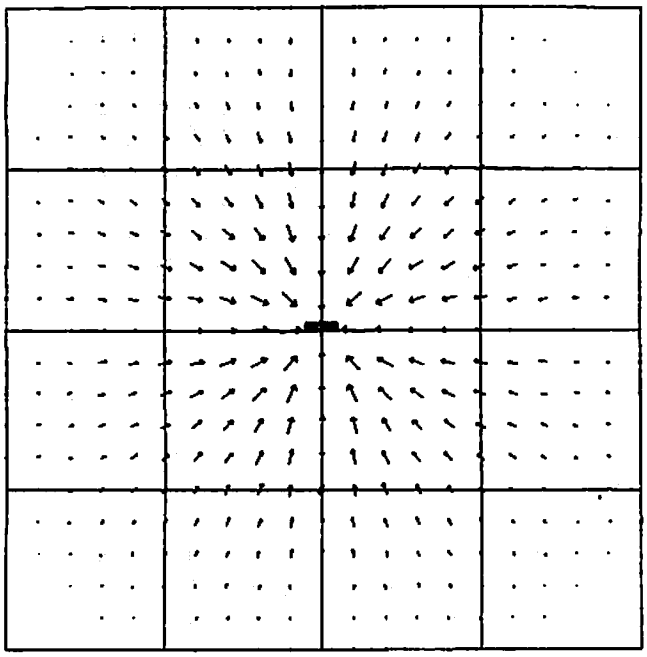

a)

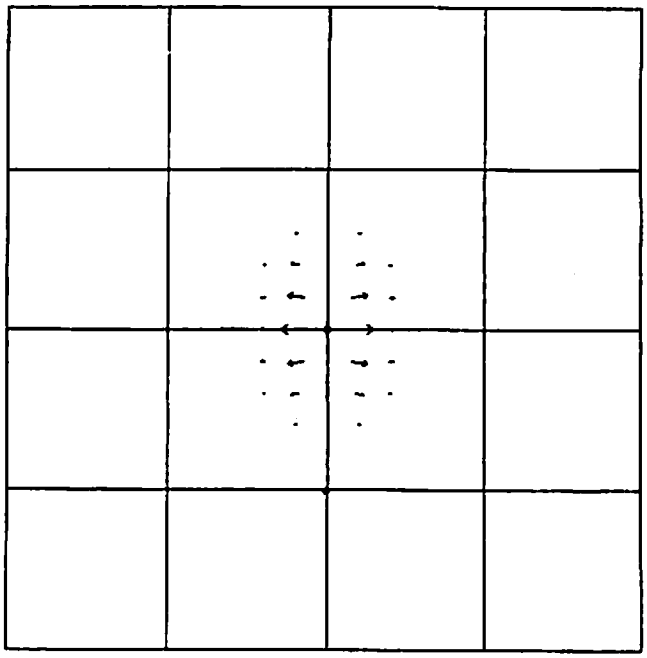

b)

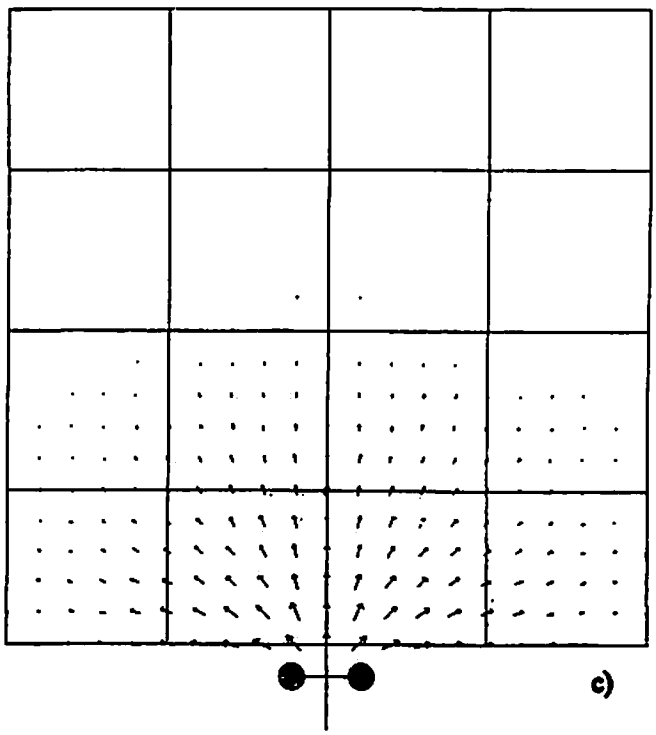

c)

Fig. 14 -- Vector Field Model, Primitive Fields

The vector field model envisions objects in the animal's visual world as determining a space of potential motor activities. The fields depicted here represent a first exploratory attempt at defining a set of primitive fields which will interact in interpreting a more complex scene. (a) A single prey object sets up a radially symmetric attractant field whose strength decays gradually with distance from the prey. (b) A single barrier object sets up a repellant field whose effect is more localized to its point of origin than is that of the prey field. The barrier field is not radially symmetric but has a lateral component that is stronger but decays more rapidly with distance than does its opposing component. (c) The vector field model also contains a representation of the animal itself. This representation is simply the converse of the prey representation, i.e., it is radially symmetric but diverges from its point of origin.

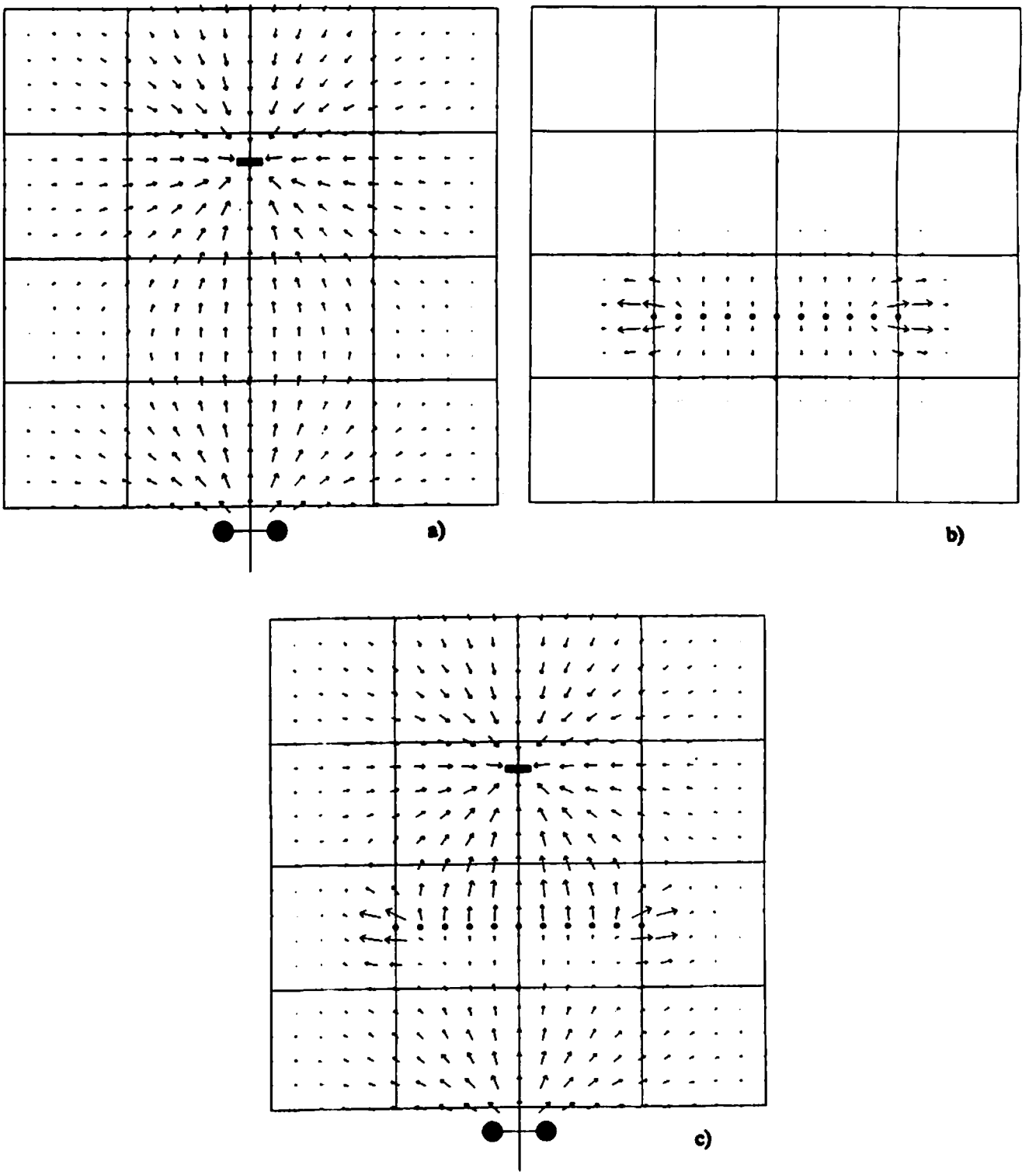
a)
b)
c)

Fig. 15 – Interaction of Primitive Vector Fields

The three types of primitive field of Figure 14 are shown here in interaction. (a) The prey attractant field in interaction with the animal's self-representation produces a field suggesting various curved paths terminating at the position of the prey. (b) The effect of the interaction of the fields from several barrier objects arranged to form a fence is to provide a strong lateral thrust at the fence ends. The lateral components produced by the interior posts is effectively cancelled by neighboring posts. c) The net field produced by the interaction of all of the elements of the configuration can be thought of as tracing out a set of paths, most of which are diverted around the fence ends.

The total field may be interpreted as representing the 'net motor effect' of the scene upon the animal, whether the animal is an essentially ballistic creature like a frog or a toad, or a more 'tracking' creature like a gerbil. In the case of the gerbil (Ingle, 1982b) we would postulate that the vector field is integrated to yield a variety of trajectories, with a weight factor for each trajectory. We would then see that this field has two 'bundles' of trajectories receiving high weight, that bundle which goes round the left end of the barrier to approach the worm, and that which goes around the right end of the barrier to approach the worm. Thus, if we change 'worm' to 'sunflower seed', we would posit that the gerbil actually builds within its brain a representation of the entire path, one of the paths is selected, and this path regulates the pattern of footfalls that will move the animal along this trajectory. In yet more sophisticated models, we could see the path not as being generated once and for all, but rather as being dynamically updated on the basis of optic flow as the animal proceeds along a chosen direction.

In toad, however, we would postulate that the vector field is processed not to yield a continuous trajectory – or a bundle of continuous trajectories of which one is to be chosen – but rather serves to generate a map of motor targets, appropriately labelled as to type. The divergence operator is a likely candidate for this form of processing. Once a suitably constructed representation of a vector field is set up, the computation of divergence is a simple local process which may be carried out in the parallel distributed fashion associated with neural mechanisms. Further, the divergence of a vector field is a scalar field. The negative of the divergence will contain peaks where the flow lines in the field tend to converge and

valleys where they tend to diverge. Figure 16 is a display of the negative of the divergence of the net field of Figure 15c. This contour indicates a trough of high divergence in front of the fence, peaks of convergence corresponding to the two edges of the fence, and a third peak corresponding to the worm. We would postulate that a scalar field of this sort could be used by motor schemas so that one of the fence ends is chosen as the motor target for a sidestep. However, the relative position of the worm is simultaneously available to determine the coordinates for the orienting schema, and for the subsequent second leg of the motor sequence that we saw to follow the pause in the trajectory shown in the right-hand side of Figure 1.

In Figure 17, we offer corresponding analyses for the cases of a fence at the position of the fence in Figure 15c but with a central gap (17a), a solid fence near to the prey (17b), a solid fence behind a fence with a gap (17c), and a cage (17d). Our research has not yet resulted in isolating the most suitable algorithm for extracting a path from data of this sort. However, these preliminary results are suggestive of a strong agreement with the behavioral data. In particular, the powerfully attractive quality of fence gaps noted by Collett (1982a, 1982b) is especially apparent.

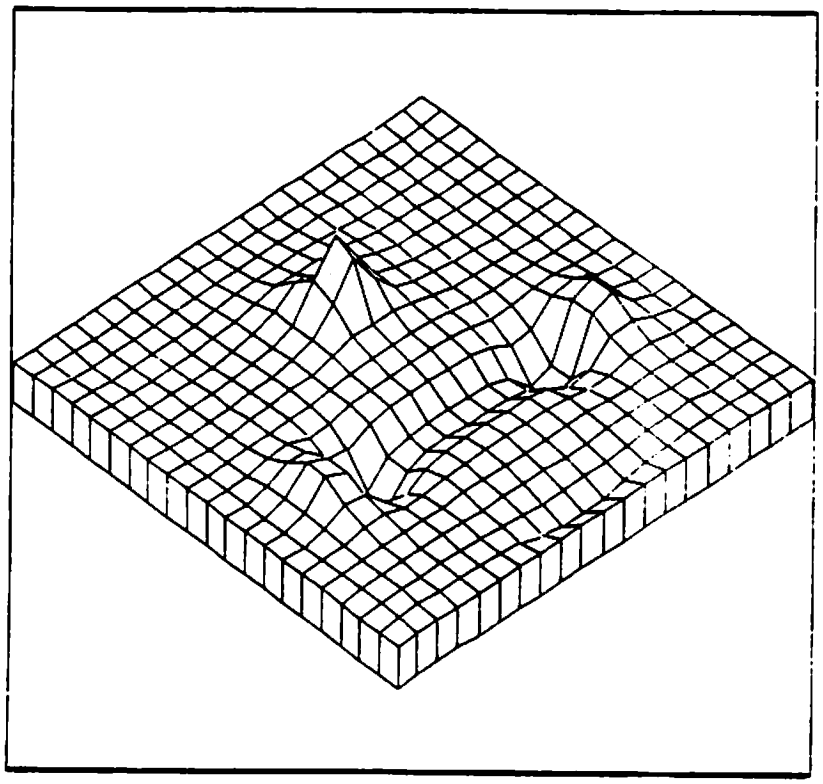

Fig. 16 – Divergence of the Net Vector Field

The negative of the divergence of the net field of Figure 15c is shown here as a 3-dimensional plot. Peaks on this plot represent regions of strong path convergence or bundling of paths, whereas valleys represent a strong divergence. The two peaks separated from each other by a trough are centered on the two fence ends. The large rear peak is centered on the prey. There is a trough of divergence in front of the fence.

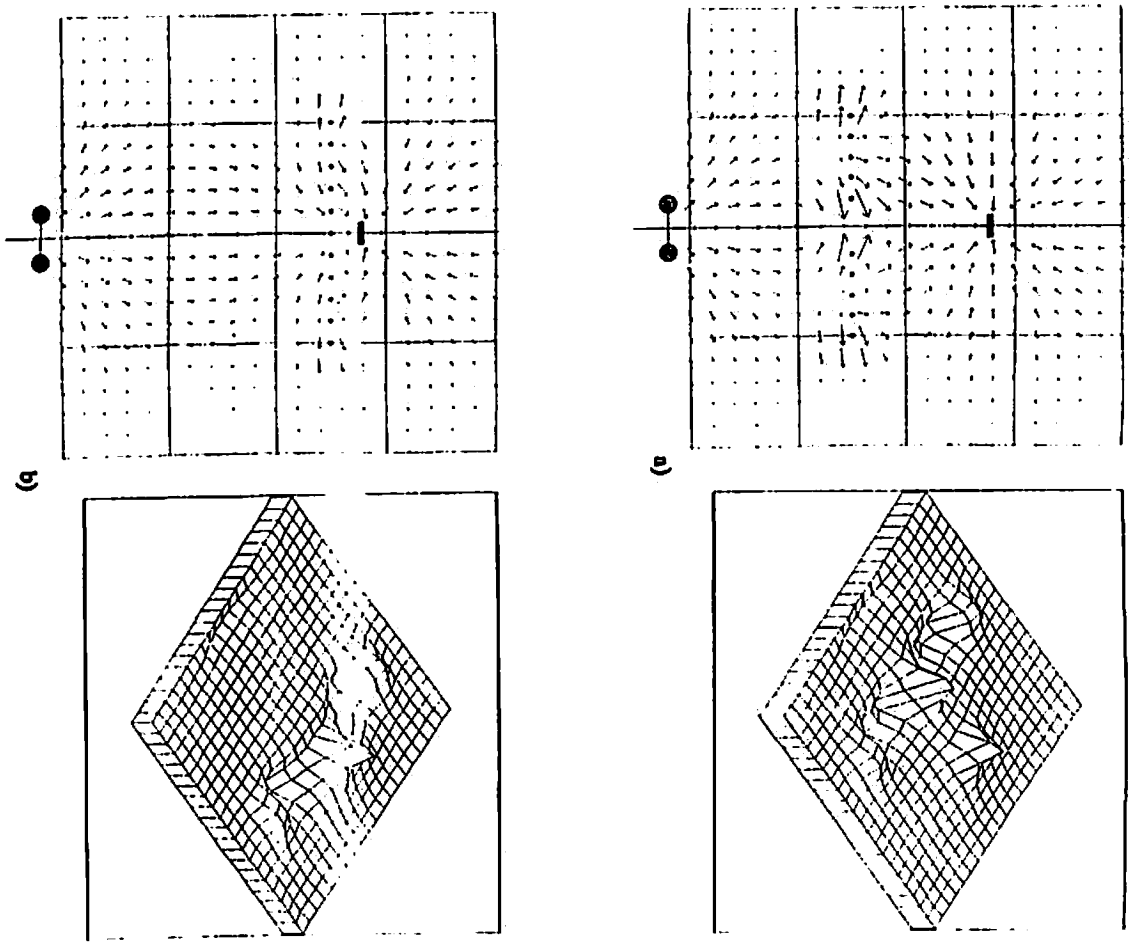
(a)
(b)
(c)
(d)

Fig. 17 – Vector Model, Comparison with Behavioral Experiments

Although an analysis has not yet been completed to identify a specific means for deriving motor activity from the vector fields, these figures indicate that the relevant information is efficiently encoded by the vector model. (a) Fence with gap. (b) Fence near to prey. (c) Fence with gap in front of a solid fence. (d) Cage. The model results are consistent with behavioral results (compare with Figure 4).

6. Discussion

The detour model of Section 4 is successful in several ways in replicating data obtained from behavioral studies. First, in the prey-barrier configurations tested it always converged upon an orientation to either a fence end or the prey. Since actual animals rarely choose any other orientation, this test is critical. Second, the selection made between a turn to a fence end or a movement towards the prey can be modulated for a variety of fence distances by a simple modification of a single model parameter – the extent of the lateral spread of prey information. This is also critical since it suggests a mechanism to explain the apparent discrepancy between the deterministic character of the computer model and the stochastic (or at least variable) character of the actual animal's response to a particular configuration.

The fact that the histogram results of the behavioral trials can be explained simply in terms of the prey-stimulus spread effect suggests the need for physiological studies of the susceptibility of tectal cell receptive field sizes to modulation based upon motivational state and experience. If receptive field sizes are prone to significant variation then the difference between the behavior of animals and this style of model will have at least one plausible source.

Several tests showed that the orientation preference of the orientation model is extremely sensitive to the position of the prey behind the barrier. When the visual input is perfectly balanced (symmetrical about the midline) the model is unable to select a single preferred orientation. However, the slightest imbalance to either side

results in an unequivocal selection of the most heavily weighted side. This suggests the need for a series of behavioral experiments to see whether or not animals also exhibit this quality. What needs to be determined is whether histograms of turn preference show a marked shift in peak orientation preference or whether there is a smooth shift in preference when the visual scene is gradually shifted from a central bias to (for instance) a left bias. Our model predicts the marked shift. An example of this sort of behavior is the 'snap zone' of frogs as reported by Ingle (1982b). Here the animal snaps at prey within the zone, orients to or hops towards prey outside the zone, and exhibits ambiguous behavior within a narrow band between the zones.

Lara et al. (1984) have offered an alternative model in the spirit of Figure 6. What is of particular interest is that they posit the recognition of gaps as an explicit step in the computation underlying detour behavior. It is thus a challenge to experimentalists to design ways to discriminate between the hypotheses that "the brain 'recognizes' barriers as inhibitory" and that "the brain 'recognizes' gaps as excitatory" in the cooperative computation of behavior. The same paper also reports models - at the level of interacting schemas, rather than layers of neuron-like elements - for prey-acquisition in environments containing chasms as well as barriers, and for predator-avoidance. Future research will test these models by developing their possible neural instantiations.

The vector model presented in Section 5 differs significantly from the simple orientation model of Section 4. The primary source of the difference is that here visual stimuli are not seen as setting up a simple decision surface which can be

processed to select among several optional actions. Rather, what is set up is a spatially encoded map of potential motor activity which in some sense is the net result of the interaction of all of the pertinent visual stimuli. Although in the simple Cartesian representation used in this paper the vectors are described in terms of components of forward and lateral motion, there is no reason to expect that the nervous system would encode vector quantities in this way. What is more likely is that they would be encoded in terms of the various types of schematized motor patterns available to the animal. For instance, a particular vector could be envisioned as having components governing side stepping, turning, and snapping. The coordinate system for such a vector field would, most appropriately, be body centered rather than eye centered.

Ingle (1982b) also suggests a model for detour behavior based upon principles similar to those employed in our simple orientation model. In this model he envisions wide-field tectal neurons driven by retinal prey detectors as providing the kind of spread effect we hypothesised in our model. He proposes that if inhibition from pretectal cells driven by barrier detectors is sufficient to suppress excitation in narrow-field tectal neurons, the effect of the wide-field neurons will be to provide a lateral shift of the locus of tectal excitation. This shift in locus would then be translated into a corresponding shift in orientation turning angle. However, his model is of a quite different character from either of the ones which we propose. He has shown that pretectum governs side stepping and tectum governs orientation turning and snapping. This has led him to suggest that the signals to the motor area from tectum and pretectum are of the nature of commands which are intended

to be executed in a coordinated way by the motor area. In our models, however, we see these signals as describing a field of potential motor activity which contains within it a spatial model of the animal's visual world. We would agree with Ingle's placement of the barrier related field in pretectum and that associated with prey in tectum. Further, we agree that final processing and decision making based upon this kind of scheme must take place in the motor area. However, we differ in that we do not see the nature of this process being to select among and coordinate independent motor commands. Rather, we see it as being a process of deriving appropriate motor responses based upon a set of spatially distributed motor cues which already contain within themselves the results of an interaction among the various visual cues.

In apparent confirmation of the notion of the global interaction embodied, especially, in our vector model is the report of Grobstein et al. (1982). Their findings indicate that tectal locus cannot be the unique determiner of orientation preference. For instance, lesions to the tectum abolish visually guided orientation turning but leave orientation to tactile stimuli intact. Conversely, lesions to the *lateral torus semicirculus* abolish tactile orientation but do not affect visual orientation. More dramatically, they have shown that small lesions of the neuraxis do not produce orientation scotomas but, rather, result in inaccurate turning and undershooting throughout the disturbed hemifield. Their conclusion is that these small lesions do not destroy linkages between particular tectal loci and turn-generating circuits but produce a more global disturbance for all tectal regions ipsilateral to the lesion.

If the vector model is to adequately represent spatially directed activity, the vector field set up by the fence posts should probably be represented by a field which survives translation of the toad's position within the field. The present model does not account for this since the fence post field shape depends upon the position of the toad -- this is in contrast to the prey field which is radially symmetric about the prey's position. Further studies with the model are needed to correct this.

REFERENCES

Amari, S. and M. A. Arbib, 1977. Competition and cooperation in neural nets. In: *Systems Neuroscience* (J. Metzler, Ed.), pp. 119-165. New York: Academic Press.

Arbib, M.A., 1981. Perceptual structures and distributed motor control. In: *Handbook of Physiology – The Nervous System II. Motor Control* (V.B. Brooks, Ed.), pp. 1449-1480. Bethesda: Amer. Physiological Society.

Caine, H.S. and E.R. Gruberg, 1985, in press. Ablation of Nucleus Isthmi Leads to Loss of Specific Visually Elicited Behaviors in the Frog, *Rana Pipiens*, *Neuroscience Letters.*

Cervantes, F., R. Lara, and M. A. Arbib, 1984. A neural model subserving prey-predator discrimination and size preference in anuran amphibia. *J. Theor. Biol.*. 113:117-152.

Collett, T., 1977. Stereopsis in toads. *Nature.* 267:349-351.

Collett, T., 1982a. Picking a route: Do toads follow rules or make plans? In *Proceedings of the Workshop on Visuomotor Coordination in Frog and Toad: Models and Experiments*, Tech. Report 82-16, Computer and Information Science Dept., Univ. of Massachusetts, Amherst.

Collett, T., 1982b. Do toads plan routes? A study of the detour behavior of *Bufo viridis*. *J. comp. Physiol.* 146:261-271

Collett, T., and S. Udin, 1983. The role of the toad's nucleus isthmi in prey-catching behavior. In *Proceedings of the Second Workshop on Visuomotor Coordination in Frog and Toad: Models and Experiments*, Tech. Report 83-19, Computer and Information Science Dept., Univ. of Massachusetts, Amherst.

Dev, P., 1975. Perception of depth surfaces in random-dot stereograms: A neural model. *Int. J. Man-Machine Studies.* 7:511-528.

Didday, R.L., 1970. The Simulation and Modelling of Distributed Information Processing in the Frog Visual System. Ph.D. Dissertation, Stanford University.

Didday, R.L., 1976. A model of visuomotor mechanisms in the frog optic tectum. *Math. Biosci.* 30:169-180.

Epstein, S., 1979. Vermin Users Manual. Unpublished project report, Computer and Information Science Dept., Univ. of Massachusetts, Amherst.

Ewert, J.-P., 1976. The visual system of the toad: behavioral and physiological studies on a pattern recognition system. In *The Amphibian Visual System A Multidisciplinary Approach* (K. Fite, Ed.), pp. 141-202. New York: Academic Press.

Grobstein, P., C. Comer, and S. K. Kostyk, 1982. Frog prey capture behavior: between sensory maps and directed motor output. In: *Proceedings of the Workshop on Visuomotor Coordination in Frog and Toad: Models and Experiments*, Tech. Report 82-16, Computer and Information Science Dept., Univ. of Massachusetts, Amherst.

House, D. H., 1982. The frog/toad depth perception system – a cooperative/competitive model. In: *Proceedings of the Workshop on Visuomotor Coordination in Frog and Toad: Models and Experiments*, Tech. Report 82-16, Computer and Information Science Dept., Univ. of Massachusetts, Amherst.

House, D. H., 1984. Neural Models of Depth Perception in Frogs and Toads. Ph.D. Dissertation, University of Massachusetts.

Ingle, D., 1976. Spatial visions in anurans. In *The Amphibian Visual System A Multidisciplinary Approach* (K. Fite, Ed.), pp. 119-140. New York: Academic Press.

Ingle, D., 1977. Detection of stationary objects by frogs (Rana pipiens) after ablation of the optic tectum. *J. Comp. Physiol. Psychol.* 391:1359-1364.

Ingle, D., 1982a. Visual mechanisms of optic tectum and pretectum related to stimulus localization in frogs and toads. In *Advances in Vertebrate Neuroethology* (J.-P. Ewert, R.R. Capranica, and D.J. Ingle, Eds.), pp. 177-226. London: Plenum Press.

Ingle, D., 1982b. The organization of visuomotor behaviors in vertebrates. In: *The Analysis of Visual Behavior* (D. Ingle, M. Goodale, and R. Mansfield, Eds.), pp. 67-109. Cambridge: MIT Press.

Jordan, M., G. Luthardt, Chr. Meyer-Naujoks, G. Roth, 1980. The role of eye accommodation in the depth perception of common toads. *Z. Naturforsch.* 35c:851-852.

Julesz, B., 1971. *Foundations of Cyclopean Perception.* Chicago: University of Chicago Press.

Lara, R., and M. A. Arbib, 1982. A neural model of interaction between tectum and pretectum in prey selection. *Cognition and Brain Theory.* 5:149-171.

Lara, R., M. Carmona, F. Daza and A. Cruz, 1984. A Global Model of the Neural Mechanisms Responsible for Visuomotor Coordination in Toads, *J. Th. Biol. 110,* 587-618.

Lara, R., F. Cervantes, and M. A. Arbib, 1982. Two-dimensional model of retinal-tectal-pretectal interactions for the control of prey-predator recognition and size preference in amphibia. In: *Competition and Cooperation in Neural Nets* (S. Amari, and M.A. Arbib, Eds.), Lecture Notes in Biomathematics *45,* pp. 371-393. Springer-Verlag.